



Terahertz modulator a using CsPbBr₃ perovskite quantum dots heterostructure

Li Shao-he¹ · Li Jiu-sheng¹

Received: 12 October 2018 / Accepted: 29 October 2018 / Published online: 7 November 2018
© Springer-Verlag GmbH Germany, part of Springer Nature 2018

Abstract

A novel terahertz wave modulator based on CsPbBr₃ perovskite quantum dots heterostructure is proposed. An external modulated 450 nm pumping laser is utilized to generate photoexcited free carriers at the CsPbBr₃ perovskite quantum dots heterostructure medium. We measured an amplitude modulation of the terahertz transmission in the frequency range from 0.23 to 0.35 THz with various laser intensity irradiances. In addition, dynamic amplitude modulation at 0.27 THz carrier wave show that the modulator provides a modulation speed of 2.5 MHz at a external pump laser irradiance of 2.0 W/cm². Our CsPbBr₃ perovskite quantum dots heterostructure can high speed modulation and can be used for terahertz modulation in addition to photovoltaics application.

1 Introduction

Terahertz waves are considered as the electromagnetic spectrum which frequency ranges from 0.1 to 10 THz, lying between the microwave and infrared regions. With the commercialization of terahertz wave sources and detectors, terahertz wave attracted significant attention because of the unique properties of terahertz radiation and has been extensively investigated. In recent years, there have been a growing interest in the development of the terahertz wave technology which has explored many potential applications in security screening, military detection, radio astronomy, high-bit-rate free-space communication, material science, nondestructive imaging, chemical and biological sensing, and medical diagnosis [1–4]. These interests have highlighted the need for numerous functional devices and components for controlling and manipulating terahertz waves, many of which are still lacking. More recently, as a dispensable device for information processing at terahertz wave communication and surveillance, terahertz wave modulator has become a hot pursuit. There have reported various approaches for the development of terahertz wave modulators such as mechanical chopper [5], liquid crystal [6], two-dimensional electron gas [7], photonic crystals

[8], semiconductor-based metamaterials [9–11], graphene [12–14], phase transition materials [15], and organic materials [16–20]. For example, Wen et al. [21] proposed all-optical graphene terahertz modulator with modulation speed of 200 kHz. Rodriguez et al. [22] designed all-electronics graphene terahertz modulator with modulation speed of 4 kHz. Unlu et al. [23] fabricated a terahertz modulator based on MEMS with modulation speed of 20 kHz. Liu et al. [24] measured a metamaterial/graphene terahertz modulator with modulation speed of 40 MHz. However, most of the terahertz wave modulator structures are too complex to limit their processing and applications. It has proved challenging to achieve high-speed modulation with a high modulation depth across a broad bandwidth of terahertz frequencies and is required for further research.

Recently, we note that the perovskite materials have attracted wide attention and extensively used in optoelectronic device applications including next-generation solar cells [25, 26], light-emitting diodes (LEDs) [27, 28], lasers [29], and photodetectors [30, 31] due to their outstanding optoelectronic properties, such as tunable bandgap [32–34], long carrier lifetimes, extra-long carrier transport distances, high carrier mobilities, high light absorption coefficients, low cost, and tunable optoelectronic characteristics [35–39]. Thus, CsPbX₃ quantum dots (QDs) and CsPbX₃ nanosheets have been demonstrated [40–42]. Meanwhile, owing to their unique characteristics, two-dimensional CsPbX₃ perovskites with QDs structure also offer a route for efficient manipulation of terahertz wave transmission due to the difference

✉ Li Jiu-sheng
jshli@126.com

¹ Centre for THz Research, China Jiliang University,
Hangzhou 310018, China

in their ionic nature and excellent optoelectronic properties compared with the traditional colloidal QDs. In this paper, we have proposed and demonstrated a high efficient terahertz wave modulator using CsPbBr₃ perovskite quantum dots heterostructure. The signal modulation mechanism of the terahertz wave modulator is based on the absorption of photo-induced carriers which can be controlled by an external continuous wave (CW) laser. Experimental results show that the presented terahertz wave modulator has high extinction ratio, simplicity, small size, and easy fabrication, which make our designs promising for a wide range of application, especially in terahertz imaging and communication systems.

2 Device design and fabrication

The terahertz modulator architecture was fabricated with the configuration shown in Fig. 1a. The CsPbBr₃ perovskite quantum dots deposited onto a 360 μm-thick, high-resistivity (> 1000 Ω cm) Si wafer with ~150 nm (2 ml of CsPbBr₃ precursor solution made in the first process was added into spinning toluene (10 ml) solution under vigorous stirring speed of 2000 rpm/min, and the adding rate was 0.1 ml/s.). The absorption coefficient of CsPbBr₃ perovskite is $7 \times 10^4 \text{ cm}^{-1}$ [43]. Figure 1b depicts the cross-sectional scanning electron microscopy (SEM) image of the device with the scale of 10 μm recorded by an electron microscope (JEOL, JSM-7800F, Japan). It is observed that the interface between CsPbBr₃ perovskite quantum dots. The

morphologies of the synthesized CsPbBr₃ perovskite quantum dots were further confirmed by transmission electron microscope (TEM) with the scale of 50 nm, as shown in Fig. 1c. For characterization of CsPbBr₃ perovskite quantum dots, the absorption and photoluminescence are measured by Omin λ300 grating spectrometer. Figure 1d shows that purified CsPbBr₃ perovskite quantum dots that employed centrifugation with alcohol as antisolvent exhibit highly stable and bright luminescence. The CsPbBr₃ exhibits absorption peak at 510 nm, from which the optical band energy are determined to be 2.25 eV. Figure 2 shows the schematic experimental configuration used for terahertz modulation of CsPbBr₃ perovskite quantum dots heterostructure. In our

Fig. 1 **a** Device schematic diagram, **b** cross-sectional SEM image of the device, and **c** transmission electron microscope (TEM) image of the CsPbBr₃ perovskite quantum dots, **d** optical absorption spectrum of CsPbBr₃ perovskite quantum dots

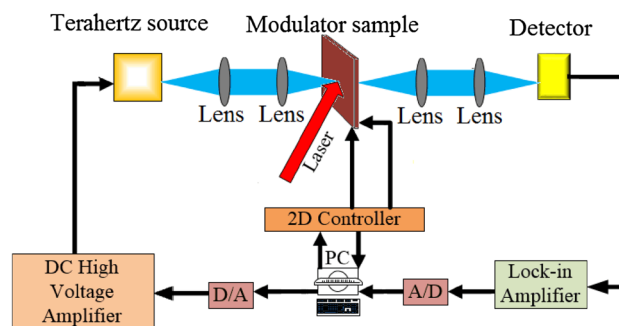
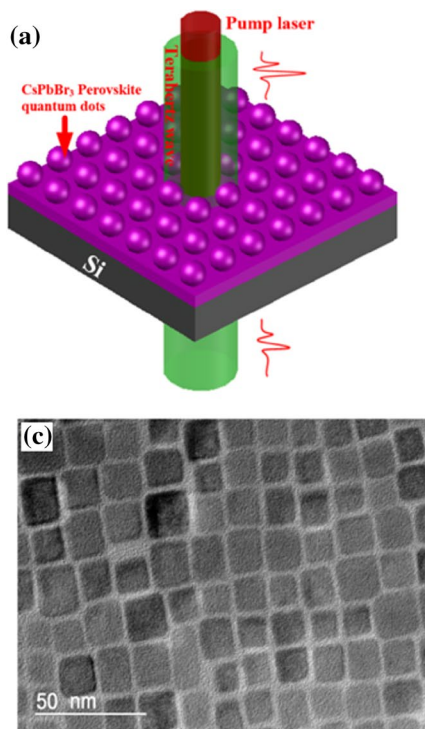


Fig. 2 Schematic diagram of the proposed terahertz wave modulator, the continuous wave terahertz wave was generated using BWO and was guided through four polymethylpentene lenses. The 450 nm continuous wave laser illuminated the surface at an oblique angle of 20°

setup, backward-wave oscillator (BWO) is a CW terahertz wave emission source, and a two-dimensional controlled stage is used to control the location of the test CsPbBr₃ perovskite quantum dots heterostructure sample. A zero-bias Schottky diode intensity detector is employed to measure the emitted terahertz power. A 450 nm continuous wave laser is mounted with a beam incident angle of 20° to the normal of the CsPbBr₃ perovskite quantum dots heterostructure. In our experiment, the laser beam is expanded. The external pump laser beam has a maximum average power of 2 W/cm² with a spot diameter of 3 mm so that it can overlap the terahertz beam diameter about 3 mm.

The spectral transmission of CsPbBr₃ perovskite quantum dot heterostructure was measured by a BWO with and without the external 450 nm pump laser excitation at the frequency range from 0.23 to 0.35 THz, respectively. The amplitude spectrum of the CsPbBr₃ perovskite quantum dots/Si under various laser intensity irradiances are depicted in Fig. 3. To investigate the modulation mechanism in detail, we deduced the optical constants of the CsPbBr₃ perovskite quantum dots/Si from the time–frequency spectral via BWO under various laser irradiances.

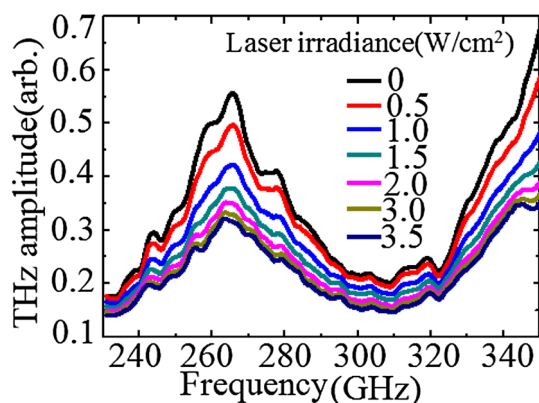


Fig. 3 Spectrum of the CsPbBr₃ perovskite quantum dots heterostructure with various laser intensity irradiances

Fig. 4 Frequency-dependent dielectric constants of the CsPbBr₃ perovskite quantum dots structure extracted by BWO. **a** Refractive index; **b** absorption coefficient

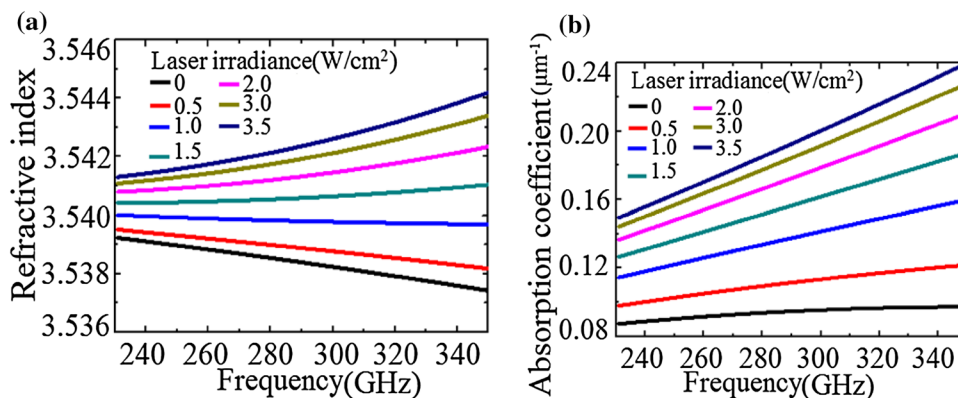


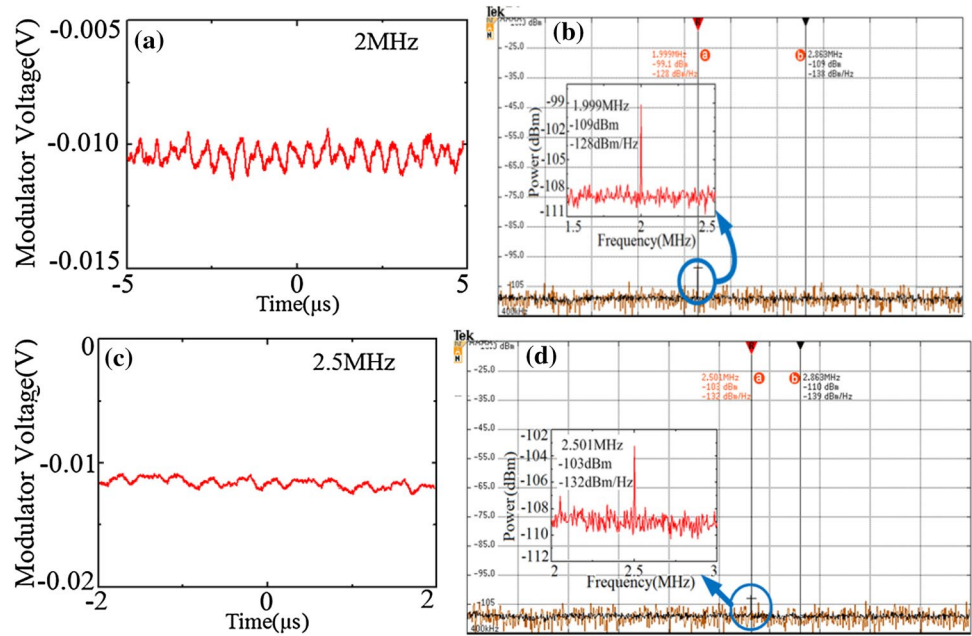
Figure 4 shows the refractive index and the absorption coefficient of CsPbBr₃ perovskite quantum dots/Si hybrid structure. The CsPbBr₃ perovskite quantum dots can form a heterostructure with semiconductor Si due to their difference in bandgap and Fermi level. When the CsPbBr₃ perovskite quantum dots/Si hybrid structure is under pump laser illumination, the photoexcited electrons and holes near the junction area are separated each other and drifted into different regions under the function of built-in electric field. Guided by previous work [44, 45], the Fermi level of perovskite quantum dot is different from that of silicon, and their valence band top and conduction band bottom are different. Then, p–n heterojunction (n perovskite, p type silicon) is formed on the interface, and the internal electric field is built due to the electron–hole drift diffusion equilibrium. Since the photo-carrier mobility of perovskite (on the order of 10) is a factor of ~ 100 less than that of silicon (on the order of 10³), causing an accumulation of photo-carriers at the CsPbBr₃ perovskite quantum dots/silicon interface, subsequently, an increase in the terahertz wave photo-induced absorption. Higher concentration of carriers can be aggregated under this mechanism and finally realize a high modulation-depth. This can be explained by the fact that the photo-doping on CsPbBr₃ perovskite quantum dots/Si hybrid structure by external pump laser in our experiment changed the dielectric property.

Taking into account an arbitrary number of multiple reflections Fabry–Perot within the sample, the transmission coefficient of the substrate and CsPbBr₃ combined is given by

$$T(\omega) = A \cdot \sum_{FP=0}^N \left(\exp(2jn(\omega)k_0d) \frac{n(\omega) - 1}{n(\omega) + 1} (2n(\omega) \cdot X - 1) \right)^{FP} \tag{1}$$

where $A = \frac{4X \cdot n(\omega)}{n(\omega) + 1} \exp(-j(n(\omega) - 1)k_0d)$, k_0 is the free space wave number, $X - 1 = 1 + n(\omega) + \sigma(\omega)Z_0$, and Z_0 is the free space impedance. Since the CsPbBr₃ layer is much less than the terahertz wavelength, CsPbBr₃ must be considered as a

Fig. 5 Modulated terahertz beam signal for a carrier wave frequency of 0.27 THz with different modulation frequency



boundary condition with a surface conductivity $\sigma(\omega)$ as follows [46]

$$\sigma(\omega) = \left[\frac{4 \cdot n(\omega)}{T(\omega) \cdot (n(\omega) + 1)} \exp(-j(n(\omega) - 1)k_0d) - 1 - n(\omega) \right] / Z_0 \quad (2)$$

When Fabry–Perot resonance takes an integer value, then Eq. (2) must be solved numerically in terms of the surface conductivity. As shown in Fig. 4, one sees that the real part of the refractive index of the CsPbBr₃ perovskite quantum dots/Si hybrid structure increases a little as the laser irradiance increases (see Fig. 4a), but the absorption coefficient of the CsPbBr₃ perovskite quantum dots/Si hybrid structure sharply increases from 0.08 to 0.24 μm^{-1} at the frequency range from 0.23 to 0.35 THz, causing the corresponding high terahertz modulation. According to the Drude model, the frequency dependent complex dielectric constant in CsPbBr₃ perovskite quantum dots/Si hybrid structure is given by $\tilde{\epsilon}(\omega) = \epsilon_\infty + \frac{i\sigma}{\omega\epsilon_0} = \epsilon_\infty - \frac{\omega_{pe}^2}{\omega(\omega + i\Gamma_e)} - \frac{\omega_{ph}^2}{\omega(\omega + i\Gamma_h)}$, where ϵ_∞ is the contribution of the dielectric and the parameter indices e and h refer to electrons and holes, respectively. $\Gamma_{e/h} = 1/\tau_{e/h}$ is the damping rate with $\tau_{e/h}$ the average collision time. The plasma angular frequency $\omega_{p(e/h)}$ is defined by $\omega_{p(e/h)}^2 = Ne/\epsilon_0 m_{e/h}$, where N is the carrier density, e is the electronic charge, ϵ_0 is the free-space permittivity, and $m_{e/h}$ is the effective carrier mass. The damping rate $\Gamma_{e/h}$ is obtained from the mobility by $\Gamma_{e/h} = e/(m_{e/h}\mu_{e/h})$. Without laser irradiance, the carrier density in CsPbBr₃ perovskite quantum dots/Si interface is very low, and the dielectric constant of CsPbBr₃ perovskite quantum dots/Si hybrid structure is real number and equals to ϵ_∞ . When the CsPbBr₃

perovskite quantum dots/Si is optically excited, a large number of free carriers are generated and then high free carrier concentrations are accumulated at the interface between silicon and quantum dots. That is to say, when the numerical value of $\omega_{p(e/h)}^2$ is larger than that of $\omega^2 + \omega\Gamma_{e/h}$, the real part of the dielectric constant in CsPbBr₃ perovskite quantum dots/Si interface becomes negative. At this time, the imaginary part of the dielectric constant in CsPbBr₃ perovskite quantum dots/Si hybrid structure can not be ignored. Since the imaginary part of the dielectric constant is corresponding to the absorption coefficient, the transmission terahertz wave is attenuated.

3 Experimental results

Here, we used the measurement set-up (see Fig. 2) for dynamic modulation characteristics test of the proposed device. The system consists of a Microtech Instruments BWO continuous wave terahertz source with a central output in the 270 GHz, and a 230–400 GHz zero-bias Schottky diode intensity detector. The average output power of the terahertz source is 10 mW. In this measurement, a square-wave voltage was used to drive the 450 nm CW diode laser to produce pump beam with the power alternating between zero and 2 W/cm². The modulator sample is placed in front of an open-ended BWO waveguide, and the transmitted signals are measured with a Schottky diode intensity detector. Figure 5 shows the detected modulation speed voltage signal of the presented terahertz wave modulator for different modulation frequencies at room temperature of 25 °C (The terahertz wave frequency is set to be 0.27 THz). From Fig. 5a,

c, one sees that the transmission amplitude of terahertz wave decreases with the increase of modulation frequency. The detected energy spectra (Tektronix Signal, Spectrum, and Modulation Analyzers) are plotted in Fig. 5b, d for different modulation frequencies. As illustrated in Fig. 5b, the power of the modulation signal peak is -109 dBm, which is larger than that of the noise power of the absorption peaks about 10 dBm. At 2.5 MHz, the device still has a response to the photoexcitation with signal peak power of -103 dBm but the signal larger than noise level (-132 dBm). Furthermore, as the CsPbBr₃ perovskite quantum dots absorption spectrum is broadband in nature and only silicon material is involved, our proposed modulator scheme may have practical applications in the terahertz wave integrated circuit fields.

4 Summary

We demonstrated the design, fabrication, and characterization of a terahertz wave modulator based on CsPbBr₃ perovskite quantum dots heterostructure. We measured the modulation of the terahertz transmission in the frequency range from 0.23 to 0.35 THz. The optical properties in terahertz band of the CsPbBr₃ perovskite quantum dots heterostructure are extracted via BWO system. By an external 450 nm laser pump irradiance of 2.0 W/cm², dynamic experiments at 0.27 THz evidence that CsPbBr₃ perovskite quantum dots heterostructure provides a modulation speed of 2.5 MHz and the modulation depth of 45.5% . The major advantage of this device is its high modulation efficiency, high speed, low-cost, easy integration and stability, which assure that this device can be a good candidate for future a practical terahertz wave communication system.

Acknowledgements The authors gratefully acknowledge the financial support from National Natural Science Foundation of China (Grant nos. 61871355, 61831012).

References

1. H.T. Chen, W.J. Padilla, M.J. Cich, A.K. Azad, R.D. Averitt, A.J. Taylor, A metamaterial solid-state terahertz phase modulator. *Nat. Photon.* **3**, 148 (2009)
2. P.H. Siegel, Terahertz technology in biology and medicine. *IEEE Trans. Microw. Theory Tech.* **52**, 2438 (2004)
3. H.T. Chen, S. Palit, T. Tyler, C.M. Bingham, J.M.O. Zide, J.F. O'Hara, D.R. Smith, A.C. Gossard, R.D. Averitt, W.J. Padilla, N.M. Jokerst, A.J. Taylor, Hybrid metamaterials enable fast electrical modulation of freely propagating terahertz waves. *Appl. Phys. Lett.* **93**, 091117 (2008)
4. H.T. Chen, W.J. Padilla, J.M.O. Zide, A.C. Gossard, A.J. Taylor, R.D. Averitt, Active terahertz metamaterial devices. *Nature* **444**, 597–600 (2006)
5. J. Li, J. Yao, Novel optical controllable terahertz wave switch. *Opt. Commun.* **281**, 5697–5700 (2008)
6. S. Savo, D. Shrekenhamer, W.J. Padilla, Liquid crystal metamaterial absorber spatial light modulator for THz applications. *Adv. Opt. Mater.* **2**, 275–279 (2014)
7. D. Shrekenhamer, S. Rout, A.C., C. Strikwerda, R.D. Bingham, S. Sonkusale Averitt, W.J. Padilla, High speed terahertz modulation from metamaterials with embedded high electron mobility transistors. *Opt. Express* **19**, 9968–9975 (2011)
8. L. Fekete, F. Kadlec, P. Kužel, H. Neřmec, Ultrafast opto-terahertz photonic crystal modulator. *Opt. Lett.* **32**, 680 (2007)
9. H.T. Chen, J.F. O'Hara, A.K. Azad, A.J. Taylor, R.D. Averitt, D.B. Shrekenhamer, W.J. Padilla, Experimental demonstration of frequency-agile terahertz metamaterials. *Nat. Photonics* **2**, 295–298 (2008)
10. H.T. Chen, H. Yang, R. Singh, J.F. O'Hara, A.K. Azad, S.A. Trugman, Q.X. Jia, A.J. Taylor, Tuning the resonance in high-temperature superconducting terahertz metamaterials. *Phys. Rev. Lett.* **105**, 247402 (2010)
11. N.H. Shen, M. Kafesaki, T. Koschny, L. Zhang, E.N. Economou, C.M. Soukoulis, Broadband blueshift tunable metamaterials and dual-band switches. *Phys. Rev. B* **79**, 161102(R) (2009)
12. B.S. Rodriguez, R. Yan, M.M. Kelly, T. Fang, K. Tahy, W. Hwang, D. Jena, L. Liu, H. Xing, Broadband graphene terahertz modulators enabled by intraband transitions. *Nat Commun* **3**, 780–786 (2012)
13. R. Degl'Innocenti, D.S. Jessop, Y.D. Shah, J. Sibik, J.A. Zeitler, P.R. Kidambi, S. Hofmann, H.E. Beere, D.A. Ritchie, Low-bias terahertz amplitude modulator based on split-ring resonators and graphene. *ACS Nano* **8**(3), 2548–2554 (2014)
14. M. Mittendorff, S. Li, T.E. Murphy, Graphene-based waveguide-Integrated terahertz modulator. *ACS Photonics* **4**(2), 316–321 (2017)
15. Y. Zhao, C. Chen, X. Pan, Y. Zhu, M. Holtz, A. Bernussi, Z. Fan, Tuning the properties of VO₂ thin films through growth temperature for infrared and terahertz modulation applications. *J. Appl. Phys.* **114**, 113509 (2013)
16. T. Matsui, R. Takagi, K. Takano, M. Hangyo, Mechanism of optical terahertz-transmission modulation in an organic/inorganic semiconductor interface and its application to active metamaterials. *Opt. Lett.* **38**, 4632–4635 (2013)
17. L. Zhong, B. Zhang, T. He, L. Lv, Y. Hou, J. Shen, Conjugated polymer based active electric-controlled terahertz device. *Appl. Phys. Lett.* **108**, 103301 (2016)
18. H.K. Yoo, S.G. Lee, C. Kang, C.S. Kee, J.W. Lee, Terahertz modulation on angle-dependent photoexcitation in organic/inorganic hybrid structures. *Appl. Phys. Lett.* **103**, 151116 (2013)
19. C.L. Li, Z.G. Zang, C. Han, Z.P. Hu, X.S. Tang, J. Du, Y.X. Leng, K. Sun, Highly compact CsPbBr₃ perovskite thin films decorated by ZnO nanoparticles for enhanced random lasing. *Nano Energy* **40**, 195–202 (2017)
20. C.L. Li, Z.G. Zang, W.W. Chen, Z.P. Hu, X.S. Tang, W. Hu, K. Sun, X.M. Liu, W.M. Chen, Highly pure green light emission of perovskite CsPbBr₃ quantum dots and their application for green light-emitting diodes. *Opt. Express* **24**, 15071–15078 (2016)
21. Q. Wen, W. Tian, Q. Mao, Z. Chen, W. Liu, Q. Yang, M. Sander-son, H. Zhang, Graphene based all-optical spatial terahertz modulator. *Sci. Rep.* **4**, 7409 (2014)
22. B. Sensale-Rodriguez, R. Yan, S. Rafique, M. Zhu, W. Li, X. Liang, D. Gundlach, V. Protasenko, M. Kelly, D. Jena, L. Liu, H.G. Xing, Extraordinary control of terahertz beam reflectance in graphene electro-absorption modulators. *Nano Lett.* **12**, 4518–4522 (2012)
23. M. Unlu, M. Hashemi, C. Berry, S. Li, S. Yang, M. Jarrahi, Switchable scattering meta-surfaces for broadband terahertz modulation. *Sci. Rep.* **4**, 5708 (2014)

24. P.Q. Liu, I.J. Luxmoore, S.A. Mikhailov, N.A. Savostianova, F. Valmorra, J. Faist, G.R. Nash, Highly tunable hybrid metamaterial employing split-ring resonators strongly coupled to graphene surface plasmons. *Nat. Commun.* **6**, 8969 (2015)
25. X. Li, D. Bi, C. Yi, J.D. Décoppet, J. Luo, S.M. Zakeeruddin, A. Hagfeldt, M. Grätzel, A vacuum flash-assisted solution process for high-efficiency large-area perovskite solar cells. *Science* **353**, 58–62 (2016)
26. G. Niu, X. Guo, L. Wang, Review of recent progress in chemical stability of perovskite solar cells. *J. Mater. Chem. A* **3**, 8970–8980 (2015)
27. F. Zhang, H. Zhong, C. Chen, X. Wu, X. Hu, H. Huang, J. Han, B. Zou, Y. Dong, Brightly luminescent and color tunable colloidal $\text{CH}_3\text{NH}_3\text{PbX}_3$ (X = Br, I, Cl) quantum dots: potential alternatives for display technology. *ACS Nano* **9**, 4533–4542 (2015)
28. H. Yoon, H. Kang, S. Lee, J. Oh, H. Yang, Y. Do, Study of perovskite QD down-converted LEDs and six-color white LEDs for future displays with excellent color performance. *ACS Appl. Mater. Interfaces* **8**, 18189–18200 (2016)
29. H. Zhu, Y. Fu, F. Meng, X. Wu, Z. Gong, Q. Ding, M.V. Gustafsson, M.T. Trinh, S. Jin, X.Y. Zhu, Lead halide perovskite nanowire lasers with low lasing thresholds and high quality factors. *Nat. Mater.* **14**, 636–642 (2015)
30. Y. Lee, J. Kwon, E. Hwang, C.H. Ra, W.J. Yoo, J.H. Ahn, J.H. Park, J.H. Cho, High-performance perovskite-graphene hybrid photodetector. *Adv. Mater.* **27**, 41–46 (2015)
31. H.R. Xia, J. Li, W.T. Sun, L.M. Peng, Organohalide lead perovskite based photodetectors with much enhanced performance. *Chem. Commun.* **50**, 13695–13697 (2014)
32. S. Stranks, G. Eperon, G. Grancini, C. Menelaou, M. Alcocer, T. Leijtens, L. Herz, A. Petrozza, H. Snaith, Electron–hole diffusion lengths exceeding 1 micrometer in an organometal trihalide perovskite absorber. *Science* **342**, 341–344 (2013)
33. S. Veldhuis, P. Boix, N. Yantara, M. Li, T. Sum, N. Mathews, S. Mhaisalkar, Perovskite materials for light-emitting diodes and lasers. *Adv. Mater.* **28**, 6804–6834 (2016)
34. N. Jeon, J. Noh, W. Yang, Y. Kim, S. Ryu, J. Seo, S. Seok, Compositional engineering of perovskite materials for high-performance solar cells. *Nature* **517**, 476–480 (2015)
35. Q. Dong, Y. Fang, Y. Shao, P. Mulligan, J. Qiu, L. Cao, J. Huang, Solar cells. Electron hole diffusion lengths > 175 nm in solution-grown $\text{CH}_3\text{NH}_3\text{PbI}_3$ single crystals. *Science* **347**, 967–970 (2015)
36. C. Wehrenfennig, G.E. Eperon, M.B. Johnston, H.J. Snaith, L.M. Herz, High charge carrier mobilities and lifetimes in organolead trihalide perovskites. *Adv. Mater.* **26**, 1584–1589 (2014)
37. A. Chanana, Y. Zhai, S. Baniya, C. Zhang, Z.V. Vardeny, A. Nahata, Colour selective control of terahertz radiation using two-dimensional hybrid organic inorganic lead-trihalide perovskites. *Nat. Commun.* **8**, 1328 (2017)
38. X. Wu, M.T. Trinh, D. Niesner, H. Zhu, Z. Noman, J.S. Owen, O. Yaffe, B.J. Kudisch, X.Y. Zhu, Trap states in lead iodide perovskites. *J. Am. Chem. Soc.* **137**, 2089–2096 (2015)
39. D.B. Mitzi, C.A. Feild, W.T.A. Harrison, A.M. Guloy, Conducting tin halides with a layered organic-based perovskite structure. *Nature* **369**, 467–469 (1994)
40. Q. Akkerman, V. D’Innocenzo, S. Accornero, A. Scarpellini, A. Petrozza, M. Prato, L. Manna, Tuning the optical properties of cesium lead halide perovskite nanocrystals by anion exchange reactions. *J. Am. Chem. Soc.* **137**, 10276–10281 (2015)
41. S. Sun, D. Yuan, Y. Xu, A. Wang, Z. Deng, Ligand-mediated synthesis of shape controlled cesium lead halide perovskite nanocrystals via reprecipitation process at room temperature. *ACS Nano* **10**, 3648–3657 (2016)
42. D. Zhang, S. Eaton, Y. Yu, L. Dou, P. Yang, Solution-phase synthesis of cesium lead halide perovskite nanowires. *J. Am. Chem. Soc.* **137**, 9230–9233 (2015)
43. J. Maes, L. Balcaen, E. Drijvers, Q. Zhao, J. De Roo, A. Vantomme, F. Vanhaecke, P. Geiregat, Z. Hens, Light absorption coefficient of CsPbBr_3 Perovskite nanocrystals. *J. Phys. Chem. Lett.* **9**(11), 3093–3097 (2018)
44. A. Singh, A. Uddin, T. Sudarshan, G. Koley, Tunable reverse-biased graphene/silicon heterojunction Schottky diode sensor. *Small* **10**(8), 1555–1565 (2014)
45. J. Ahn, H. Park, M.A. Mastro, J.K. Hite, C.R. Eddy Jr., J. Kim, Nanostructured n-ZnO/thin film p-silicon heterojunction light-emitting diodes. *Opt. Express* **19**(27), 26006–26010 (2011)
46. M. Liang, Z.R. Wu, L.W. Chen, L. Song, P. Ajayan, H. Xin, Terahertz characterization of single-walled carbon nanotube and graphene on-substrate thin films. *IEEE Trans. Microw. Theory Tech.* **59**, 2719–2725 (2011)